Journal of Sound and Vibration (2002) **256**(1), 155–171
doi:10.1006/jsvi.5202, available online at http://www.idealibrary.com on IDEAL®

AN ESTIMATOR-BASED SLIDING-MODE CONTROL FOR MANEUVERING A FLEXIBLE SPACECRAFT

Y.-G. SUNG

Department of Mechanical Engineering, Chosun University, 375 Seosuk-dong Dong-gu, Kwangju, 501-759, Korea. E-mail: sungyg@chosun.ac.kr

(*Received* 25 *October* 2000, *and in final form* 9 *October* 2001)

An estimator-based sliding-mode controller (ESMC) is discussed for a linear stochastic system with a known disturbance and is utilized in a flexible spacecraft for the reduction of residual vibration while allowing natural deflection during operation. By converting the tracking problem into a regulator problem, the ESMC minimizes the expected value of the guadratic objective function composed of errors which always remain in the intersection of sliding hypersurfaces. For the numerical evaluation to take place in a flexible with a flexible spacecraft, a large slewing maneuver strategy is devised, with a tracking model for the nominal trajectory. A start-coast-stop strategy for an economical maneuver is employed in conjunction with the input shaping technique. The performance and efficacy of the proposed control scheme are illustrated with a comparison of different maneuvering strategies.

1. INTRODUCTION

In future generations of flexible spacecraft, an appropriate, reliable control system design will be a challenging problem because of its special dynamic characteristics which include a large number of significant elastic modes with very small, inherent, damping inaccuracies in the area of system parameters and non-linear effects. The control methods are related to multi-input, multi-output (MIMO) configurations. As a result, it is natural to use an optimal formulation in order to design an effective controller. However, due to the conditions of a space operation, stringent stability and robustness are required. In order to satisfy these requirements, many algorithms have been proposed by employing optimal control, adaptive control, sliding-mode control (SMC), etc.

SMC has been used extensively in robotics [1], in which information is readily available. Slotine proposed a boundary layer concept to reduce the chattering problem by introducing a linear function within the switching region. In the application of the SMC to flexible structures, Öz and Mostafa [2] investigated switching mechanisms, stability, interaction with unmodelled dynamics, and the chattering problem with general non-linear systems. They determined that the chattering issue is not the main obstacle of the application to the SMC, but found that truncation effects are problematic. Young and Özguner [3] combined the SMC with a frequency weighted optimal formulation [4] to reduce the chattering due to rapid switching logic. Sinha and Miller [5] proposed an optimal SMC with a Kalman filter to reject stochastic broadband torque disturbances. As a matter of fact, Utkin initially developed SMCs for multi-variable cases by making the optimal cost functional. It is possible to combine the SMC with an estimator, as long as

0022-460X/02/$35.00

state estimation is asymptotically convergent to the true states [6]. However, an estimator-based SMC has not been adequately addressed or discussed.

In this paper, an estimator-based sliding-mode controller (ESMC) is initially presented for a linear stochastic system with known disturbances. In the following sections, an analysis of the dynamics of a closed-loop system is discussed, as well as the constant optimal gain selection of hypersurfaces. The robustness and interaction by unmodelled dynamics is also considered. Secondly, in the numerical application of the ESMC to the Spacecraft Control Laboratory Experiment (SCOLE) model, a tracking model is presented with an arbitrary influence vector, which is chosen by the control system designer. A maneuvering strategy is discussed for efficient control implementation in conjunction with an input shaping technique. In the worst case scenario for the control scheme, the extreme case, with no damping effect, is discussed relative to the performance of the ESMC.

2. ESTIMATOR-BASED SLIDING-MODE CONTROLLER

Consider a linear stochastic system with such known disturbances

$$\dot{z}(t) = A\,z(t) + B\,u(t) + L\,w(t) + D(t), \tag{1}$$

$$y(t) = C\,z(t) + v(t) \tag{2}$$

where the state vector is $z(t) \in \mathbf{R}^k$, the input vector is $u(t) \in \mathbf{R}^m$, and the output vector is $y(t) \in \mathbf{R}^l$. $D(t)$ contains known disturbances which can be non-linear functions. It is assumed that (A, B) and (A, C) are controllable and observable respectively. The plant disturbance vector $w(t)$ and the sensor noise vector $v(t)$ contain independent white-noise processes with a zero mean, as their elements. Their covariance matrices can be defined as

$$\mathbf{E}[w(t)\,w(\tau)^{\mathrm{T}}] = Q\,\delta(t-\tau), \tag{3}$$

$$\mathbf{E}[v(t)\,v(\tau)^{\mathrm{T}}] = R\,\delta(t-\tau), \tag{4}$$

where $\delta(t-\tau)$ is the Dirac delta function.

The estimator dynamics for state estimation can be expressed as

$$\dot{\hat{z}}(t) = A\,\hat{z}(t) + B\,u(t) + D(t) + K_f\,[y(t) - C\,\hat{z}(t)], \tag{5}$$

where the Kalman gain K_f is obtained by

$$K_f = P\,C^{\mathrm{T}}R^{-1}, \tag{6}$$

$$\dot{P} = P\,A^{\mathrm{T}} + AP + Q - PC^{\mathrm{T}}\,R^{-1}\,CP. \tag{7}$$

If the prescribed configuration vector $z^*(t)$ is considered, the configuration error vector can be expressed as

$$z_e(t) = \hat{z}(t) - z^*(t). \tag{8}$$

Introducing $\hat{z}(t) = z_e(t) + z^*(t)$ into equation (5), the error dynamics are expressed in terms of the error state vector $x_e(t)$.

$$\dot{z}_e(t) = A\,z_e(t) + B\,u(t) + D(t) + K_f\,[y(t) - C\,z_e(t)\,] - \dot{z}^*(t). \tag{9}$$

The m hypersurfaces, passing through the origin of the error state space, are defined as

$$s_i(t) = g_i^{\mathrm{T}}\,z_e(t), \quad i = 1, 2, \ldots, m. \tag{10}$$

The control consists of a *reaching phase*, in which the system moves from its initial position in the state space to the sliding surface, and a *sliding phase*, in which it moves along the sliding surface to the origin. The sliding surface *attractivity condition* is typically defined as

$$s_i(t)\,\dot{s}_i(t) \leqslant 0, \quad i = 1, 2, \ldots, m. \tag{11}$$

The attractivity condition and the error dynamics equation (9) yield the equivalent controller, defined as the solution of $\dot{s}_i(t) = 0, (i = 1, 2, \ldots, m)$:

$$u_{eq}(t) = -(GB)^{-1} G[(A - K_f C)\,\hat{z}(t) + K_f y(t) + D(t) - \dot{z}^*(t)], \tag{12}$$

where $G = [g_1,\ g_2,\ \ldots,\ g_m]$. From equation (10), the sliding surface is written as

$$S(t) = G\,z_e(t), \tag{13}$$

where $S(t) = [s_1(t),\ s_2(t),\ \ldots,\ s_m(t)]^{\mathrm{T}}$.

In fact, the equivalent control is an ideal sliding motion where $S(0) = 0$. In order to satisfy the reaching conditions, a switching logic is used for the realization of a smooth sliding motion. In practice, it can be approximated by the reaching dynamics that arbitrarily close within the limitations of the control switching devices, which are related to an infinite switching frequency of controls approximate to the ideal sliding motion. As a result, the switching logic becomes a non-ideal sliding motion which results in a chattering motion phenomenon. In the practical applications of the classical SMC for controlling flexible systems, the chatter phenomenon can excite the unmodelled flexible modes. In this paper, a global asymptotic reaching technique [7] is employed to guarantee convergence without experiencing an overshooting problem in the sliding region, so that the overall maneuver is accomplished in a smooth manner. The control law is chosen as

$$u(t) = u_{eq}(t) - (GB)^{-1} P_s S(t), \tag{14}$$

where $P_s = vI^{m\times m}$ is selected. As a result, using equations (12)–(14), the estimator-based sliding-mode control law is expressed as

$$\begin{aligned} u(t) = &-(GB)^{-1}[G(A - K_f C)\,\hat{z}(t) + P_s G z_e(t) \\ &+ GK_f\,y(t) + GD(t) - G\dot{z}^*(t)]. \end{aligned} \tag{15}$$

Take note that the control law includes direct feedback of the output, the estimated states, and the tracking trajectory.

3. ANALYSIS AND GAIN SELECTION OF THE ESMC

In this section, the dynamics in the closed-loop control system are investigated. Next, the optimal gain selection of the sliding hypersurface is discussed. Lastly, robustness is considered for chattering circumstance.

3.1. DYNAMICS OF THE CLOSED-LOOP SYSTEM

The behavior of the closed-loop system and estimator can be understood by defining the estimation error.

$$\bar{z}(t) = z(t) - \hat{z}(t). \tag{16}$$

Using equations (1) and (5), the error dynamics are expressed as

$$\dot{\bar{z}}(t) = (A - K_f C)\,\bar{z}(t) + L\,w(t) - K_f\,v(t). \tag{17}$$

In terms of $\bar{z}$, equation (15) can be written as

$$u(t) = -(G\,B)^{-1}[\{G(A - K_f\,C) + G\,K_f\,C - P_s\,G\}\,z(t) - \{G(A - K_f\,C) - P_s G\}\,\bar{z}(t) + G\,K_f\,v(t) + G\,D + P_s\,G\,z^*(t) - G\,\dot{z}^*(t)]. \tag{18}$$

Substituting equation (18) for equation (1), the closed-loop dynamics can be expressed as

$$\dot{z}(t) = [A - \Omega\,A - B(G\,B)^{-1}P_s\,G)]\,z(t) + [\Omega(A - K_f\,C) - B(G\,B)^{-1}P_s\,G]\,\bar{z}(t) + Lw(t) - \Omega\,K_f\,v(t) - B(G\,B)^{-1}\,P_s\,G\,z^*(t) + \Omega\,\dot{z}^*(t), \tag{19}$$

where $\Omega = B(GB)^{-1}G$. The closed-loop dynamics are driven by estimation error, noises, and tracking commands. Now, the augmented system of equations (17) and(19) is given as

$$\begin{Bmatrix} \dot{z}(t) \\ \dot{\bar{z}}(t) \end{Bmatrix} = \begin{bmatrix} A - \Omega\,A + \Gamma & \Omega\,(A - K_f\,C) - \Gamma \\ 0 & A - K_f C \end{bmatrix} \begin{Bmatrix} z(t) \\ \bar{z}(t) \end{Bmatrix} + \begin{bmatrix} L & -\Omega\,K_f \\ L & -K_f \end{bmatrix} \begin{Bmatrix} w(t) \\ v(t) \end{Bmatrix} + \begin{Bmatrix} -\Gamma\,x^*(t) + \Omega\,\dot{z}^*(t) \\ 0 \end{Bmatrix}, \tag{20}$$

where $\Gamma = B\,(G\,B)^{-1}\,P_s\,G$. Since the augmented system is a block triangular, the eigenvalues are those of $A - \Omega A + \Gamma$ and $A - K_f C$. It is shown that $A - \Omega A + \Gamma$ is the closed-loop plant matrix for the full-state feedback problem. As a result, the eigenvalue separation principle holds so that the controller and estimator can be independently designed.

Lemma 3.1. *The m eigenvalues of $A - \Omega A + B(GB)^{-1}P_sG)$ are decided by the $-P_s$ matrix and the remaining $k - m$ eigenvalues can be arbitrarily placed in the S-plane by a proper selection of G, since the system (A,B) is controllable.*

The proof of Lemma 3.1 can be presented in the manner of reference [6]. Let the columns of matrix Q_1 consist of the basis vectors of the null space of B^{T}. The coordinate transformation is defined by

$$\eta(t) = M\,z_e(t), \tag{21}$$

where the matrix M is composed as

$$M = \begin{bmatrix} Q_1 \\ B \end{bmatrix}. \tag{22}$$

By substituting equation (21) for equation (1) and ignoring noises, the transformed equation can be expressed as

$$\dot{\eta}(t) = \bar{A}\,\eta(t) + \bar{B}\,u(t) + \bar{D}, \tag{23}$$

where

$$\bar{A} = MAM^{-1},$$

$$\bar{B} = MB,$$

$$\bar{D} = MD. \tag{24}$$

Since the matrix M consists of the orthogonal basis of B^{T}, the first $k - m$ rows of $\bar{B}$ are zeroes. Therefore, the vector $\eta(t)$ is partitioned, such that, $\eta_1(t)$ is $k - m$ vector and $\eta_2(t)$ is m vector. The partitioned dynamic equation can be presented as

$$\dot{\eta}_1(t) = A_{11}\eta_1(t) + A_{12}\,\eta_2(t) + D_1(t), \tag{25}$$

$$\dot{\eta}_2(t) = A_{21}\,\eta_1(t) + A_{22}\,\eta_2(t) + B_r\,u(t) + D_2(t). \tag{26}$$

Then, $S(t)$ can be written as

$$\bar{S}(t) = \eta_2(t) + K_s\,\eta_1(t). \tag{27}$$

For the full-state feedback problem, the gain G is obtained by equating equation (13) with $\bar{S}$ as

$$G = \begin{bmatrix} K_s, & I^m \end{bmatrix} M. \tag{28}$$

Substituting equation (27) for equation (25) and using the global reaching technique [2], the system dynamics for the full-state feedback problem can be expressed as

$$\begin{Bmatrix} \dot{\eta}_1(t) \\ \dot{\bar{S}}(t) \end{Bmatrix} = \begin{bmatrix} A_{11} - A_{12}K_s & A_{12} \\ 0 & -P_s \end{bmatrix} \begin{Bmatrix} \eta_1(t) \\ \bar{S}(t) \end{Bmatrix} + \begin{bmatrix} D_1(t) \\ 0^{m\times 1} \end{bmatrix}. \tag{29}$$

Since the closed-loop system matrix for the full-state feedback problem is $A - \Omega A + B(GB)^{-1}P_sG$ and the eigenvalues remain unchanged under the similarity transformation, the eigenvalues of $A - \Omega A + B(GB)^{-1}P_sG$ are $k - m$ eigenvalues from $A_{11} - A_{12}K_s$ and m eigenvalues from $-P_s$. When the sliding surface, $\eta_2 = -K_s\eta_1$ eigenvalues of $A_{11} - A_{12}K_s$ can be arbitrarily placed in the S plane by a proper selection of K_s [6]. In an analysis of the closed-loop dynamics, the feedback term for the attitude control is not considered due to the negligible coordinate.

3.2. OPTIMAL GAIN OF SLIDING HYPERSURFACES

As implied in the derivation of the control law, the tracking problem is reduced to a regulator problem with full-state feedback by taking $z_e(t) = \hat{z}(t) - z^*(t)$. The idea can be used in the decision of the matrix G, which minimizes the quadratic objective function:

$$J = \int_0^\infty z_e^{\mathrm{T}}(t)\, Q_s\, z_e(t)\, \mathrm{d}t, \tag{30}$$

where Q_s is symmetric and positive semidefinite. Using equation (21),

$$J = \int_0^\infty \eta^{\mathrm{T}}(t)(M^{-1})^{\mathrm{T}} Q_s M^{-1}\eta(t)\, \mathrm{d}t. \tag{31}$$

With the property of similarity transformation, the matrix $(M^{-1})^{\mathrm{T}}Q_sM^{-1}$, which is symmetric and positive semidefinite, it is defined as

$$(M^{-1})^{\mathrm{T}}\, Q_s\, M^{-1} = \begin{bmatrix} Q_1 & N \\ N^{\mathrm{T}} & R \end{bmatrix}. \tag{32}$$

Hence, the performance index can be expressed as

$$J = \int_0^\infty (\eta_1^{\mathrm{T}}(t)\, Q_1\, \eta_1(t) + \eta_2^{\mathrm{T}}(t)R\eta_2(t) + 2\,\eta_1^{\mathrm{T}}(t)N\eta_2(t))\, \mathrm{d}t. \tag{33}$$

As a standard linear quadratic problem equation (33), the optimal feedback gain matrix [8] is written as

$$K_s = (R)^{-1}\,[\,A_{12}^{\mathrm{T}}, \quad P_2 + N^{\mathrm{T}}\,], \tag{34}$$

where

$$\begin{aligned} 0 = {} & P_2\,(A_{11} - A_{12}\,R^{-1}\,N^{\mathrm{T}}) + (A_{11}^{\mathrm{T}} - N\,R^{-1}\,A_{12}^{\mathrm{T}})\,P_2 - \\ & P_2\,A_{12}\,R^{-1}\,A_{12}^{\mathrm{T}}\,P_2 + Q_1 - N\,R^{-1}\,N^{\mathrm{T}}. \end{aligned} \tag{35}$$

The optimal gain G is obtained by substituting equation (34) for equation (28).

However, there is a question as to whether or not the choice of G minimizes the stochastic objective function, similar to the deterministic case. As long as the objective function meets the linear quadratic Gaussian problem, the optimality of J in a stochastic sense [9] is guaranteed.

3.3. ROBUSTNESS OF REACHING DYNAMICS

Due to the chattering issue of the sliding-mode controller, the controller utilizes the globally asymptotic reaching technique, based on an ideal linear model. In order to evaluate the robustness of the technique in the presence of non-ideal effects, such as parameter uncertainties, time-varying dynamics, and internal or external disturbances, one can make sure that the ideal sliding surface is guaranteed.

Equation (1) with non-ideal effects can be expressed as

$$\dot{z}(t) = A\,z(t) + B\,u(t) + \Delta f, \tag{36}$$

where Δf accounts for all non-ideal effects. If a controller is designed with a linear dynamic model using the globally asymptotic reaching technique, the control law can be stated as

$$u(t) = -(GB)^{-1}[\,P_s G + GA]\,z(t). \tag{37}$$

Now, if the control law is applied to equation (36), the *reaching condition* can be written as

$$\begin{aligned} S^{\mathrm{T}}(t)\,\dot{S}(t) &= (G\,z(t))^{T}[G\,A\,z(t) + G\,B\,u(t) + G\,\Delta f] \\ &= (G\,z(t))^{\mathrm{T}}[-P_s\,G + G\,\Delta f]. \end{aligned} \tag{38}$$

The reaching dynamics can be expressed as

$$\dot{S}(t) = -P_s\,S(t) + G\Delta f. \tag{39}$$

Therefore, the reaching dynamics is stable with Δf since $P_s > 0$. The steady-state solution of equation (39) can be expressed as

$$S_{ss} = \int_0^t \mathrm{e}^{-P_s(t-\tau)}\,G\,\Delta f\,\mathrm{d}\tau. \tag{40}$$

Hence, due to non-ideal effects, there is a steady state error as $t \to \infty$, so that it cannot reach an equilibrium point. As a rule of thumb in the sliding-mode controller design, it is possible to compensate for the error by a large matrix P_s [2].

4. APPLICATION TO THE SCOLE MODEL

The SCOLE system is shown in Figure 1 to present the bending and linear functions of axial and torsional deformations. A set of simultaneous non-linear ordinary differential equations can be found in reference [10]. By using a perturbation approach, the equations are separated into a set of equations for rigid-body motions, representing zero order effects, and a set of equations for small elastic motions and deviations from the rigid-body motions, representing first order effects. The approach in reference [10] permits a maneuvering strategy that is independent of deflection control. Based on the formulation, a control scheme in Figure 2 is designed using the ESMC.

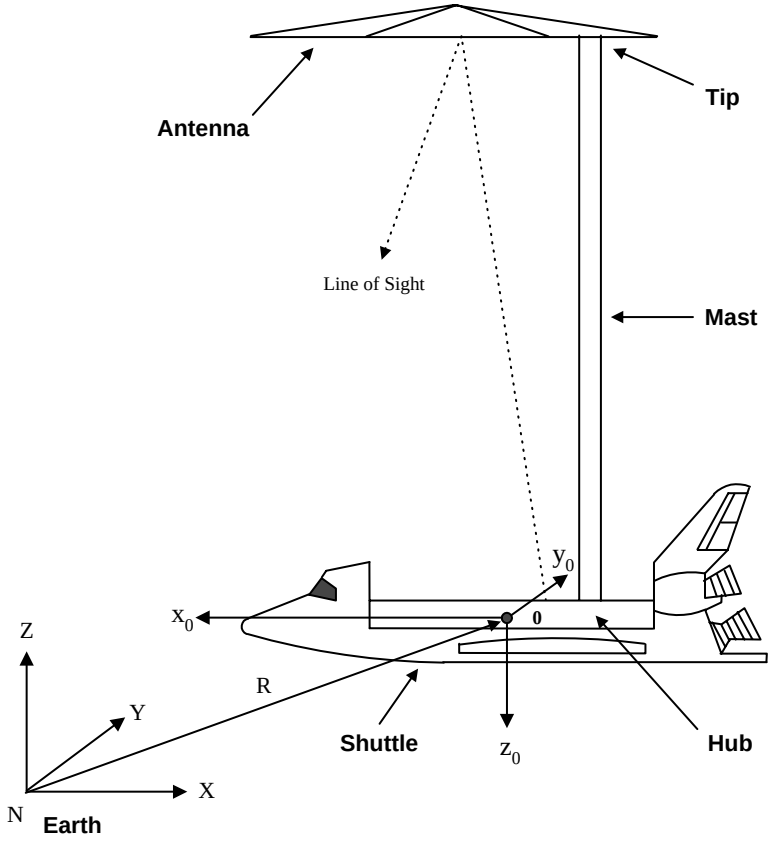

Figure 1. Spacecraft Control Laboratory Experiment configuration.

4.1. ELASTIC TRACKING MODEL

A tracking model is presented to generate the desired elastic states so that a natural deflection of the system is experienced. The structural equation of the SCOLE mast, for which the state estimator is designed, with the assumption of direct measurement of the rigid-body states, can be written as

$$\ddot{\bar{z}}_f + C_{ff}\dot{\bar{z}}_f + K_{ff}\,\bar{z}_f = F_f - D_s(\bar{z}_r, \bar{z}_f, \dot{\bar{z}}_r, \dot{\bar{z}}_f), \tag{41}$$

where $D_s(\bar{z}_r, \bar{z}_f, \dot{\bar{z}}_r, \dot{\bar{z}}_f)$ is considered as a disturbance term, which includes stiffening, gyroscopic, and coupled terms and the subscripts r and f stand for rigid- and flexible-body respectively.

The tracking model can be obtained from equation (41) by excluding time-varying matrices and internal forces, so that the tracking model provides ideal elastic states for the controller. It serves as a nominal linear trajectory for the flexible-body dynamics. Using modal analysis, transformation between the tracking model and equation (41) is obtained by

$$\bar{z}_f(t) = T z_d(t), \tag{42}$$

where $T \in \mathbf{R}^{l\times l}$ is a set of eigenvectors. The tracking model is expressed as

$$\ddot{z_d}(t) + 2\,\zeta\omega_n\,\dot{z_d}(t) + \omega_n^2\,z_d(t) = -\mu\,T^{-1}\,A_e\,\ddot{\theta}, \tag{43}$$

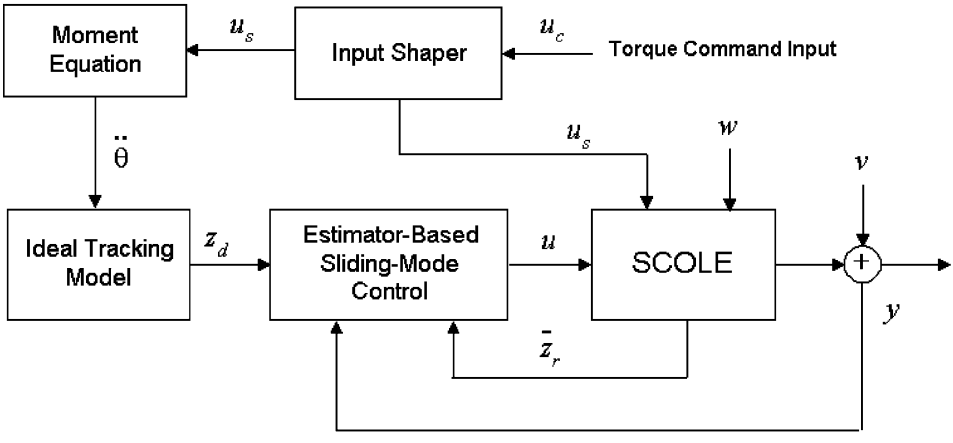

Figure 2. The closed-loop control system.

where A_e is defined as an influence matrix, obtained by the terms of equation (41) associated with $\ddot{\theta}$, which will be the designed angular acceleration element in the numerical evaluation. The ζ and ω_n are the damping coefficient and the natural frequency respectively. Hence, the right-hand side [11] of equation (43) is considered as a tangential force associated with the desired angular displacement. The μ is a scaling factor, which can be used in the case of a high angular velocity maneuver, in order to operate the system within either an elastic range or a small deflection circumstance. The tracking model equation (43) is employed for generations of desired elastic states.

4.2. START-COAST-STOP MANEUVER STRATEGY

In a rigid-body-like maneuver with zero order perturbation, each moment along the $x_0y_0z_0$ axes of the zero order perturbed moment M_0 desired to produce a rigid-body rotation about the 1 axis (not necessarily a principal axis) is expressed as

$$M_{01} = I_{11}\ddot{\theta}, \tag{44}$$

$$M_{02} = I_{21}\,\ddot{\theta} - I_{31}\,\dot{\theta}^2, \tag{45}$$

$$M_{03} = I_{31}\,\ddot{\theta} + I_{21}\,\dot{\theta}^2, \tag{46}$$

where θ is the desired angular displacement. The inertia moments [12] in the above equations are the elements of I_0, the mass moment of inertia, in relationship to the rotational axis. These moments are applied to the SCOLE to perform the slewing maneuver with respect to one axis. Instead of optimal formulation [11, 13] in order to minimize either operational time or fuel or both, which lead to solutions for two-point boundary problems, a simple operation is employed and targeted towards the reduction of operational time and fuel consumption. In this paper, the torque command input $M_{01} = u_c(t)$ for a roll maneuver around an x_0-axis in the paper used in conjunction with the input shaping technique is expressed as

$$u_c = \begin{cases} T_{amp}\sin^2 \Omega t & \text{if } t \le t_0 = \frac{\pi}{\Omega} \\ 0 & \text{otherwise,} \end{cases} \tag{47}$$

where T_{amp} is the torque magnitude and Ω is the period of the torque input profile. The input profile is used for start and stop motions. During the coasting period, no additional input is required except for control input to treat disturbances. The smooth input profile is selected because an excitation of high-frequency modes should be reduced during the transient period.

In order to accurately arrive at the desired final angle of the roll maneuver, an analytical solution for intermediate time interval is needed. By taking a time integration of equation (44) with equation (47), the desired coasting angular velocity is given as

$$\dot{\theta}_c = \frac{T_{amp}}{I_{11}}\left(\frac{t_0}{2} - \frac{\sin 2t_0}{4}\right), \tag{48}$$

where $\dot{\theta}_c$ is the coasting angular velocity of $\dot{\theta}$. If the desired final angle θ_f is given, the coasting time interval, t_c, can be stated as

$$t_c = t_0 + \frac{\theta_f}{\dot{\theta}_c}. \tag{49}$$

4.3. INPUT SHAPING

With the tracking model used to generate the desired states for the ESMC, the input shaping technique [14] is employed to provide the residual vibration-free states after the end of input in an open-loop manner. As an idea, the system to be controlled is allowed to vibrate for a one half period of time in the lowest mode. It is not necessary that the system should be held firmly to suppress the vibration of the flexible structure in the case of the rest-to-rest maneuver. With two-impulse sequences, the shaped input u_s of the desired input $u(t)$ can be written as

$$u_s(t) = A_1 u(t) + A_2 u(t - \Delta T) \tag{50}$$

in which

$$A_1 = \frac{1}{1 + K_p},$$

$$A_2 = \frac{K_p}{1 + K_p},$$

$$K_p = \mathrm{e}^{-\frac{\zeta\pi}{\sqrt{1-\zeta^2}}},$$

$$\Delta T = \frac{\pi}{\omega_n\sqrt{1 - \zeta^2}},$$

where ω_n and ζ are the vibration modal frequency and damping, respectively, of a second order modal equation. This function as a true maneuver input is applied to the tracking model and the shuttle operation of the SCOLE system for a large angle maneuver.

4.4. NUMERICAL SIMULATION

The full order model, 84 degrees of freedom, is reduced to 12 degrees of freedom including the six rigid-body modes by using the frequency-dependent Krylov vectors [15] to design the ESMC. The full order proportional damping formula used is $C_f =$

$\alpha M_f + \beta K_f$ where $\alpha = \beta = 0{\cdot}005$ is selected, but knowing that the damping factor of space structures is very small. M_f and K_f are the constant mass and stiffness matrices of the SCOLE model with zeroing the terms of rigid-body modes. A discussion of the zero damping case will be discussed at this end of the section. The first and second natural frequencies of the mast are 0·9563 and 1·0221 Hz, respectively.

For the application of the ESMC to the SCOLE model, equation (15) is expressed with the assumption of the measurable rigid-body states as

$$\begin{aligned} u(t) = & -(GB)^{-1}[G(A - K_f C)\,\hat{z}(t) + P_s G z_e(t) \\ & + \kappa G z_{re}(t) + G K_f y(t) + GD(t) - G\,\dot{z}^*(t)], \end{aligned} \tag{51}$$

where the attitude error feedback term $\kappa\, G\, z_{re}(t)$ is introduced which will be necessary for the shuttle control. $z_{re}(t)$ is only the rigid-body state error.

There are three torque and three force actuators applied to the shuttle control. The three torque wheels are mounted on the mast-tip to control vibration. In this study, it is assumed that the measured variables are θ, $\dot{\theta}$, x, and $\dot{x}$ of the shuttle. The state variables of the mast with respect to the shuttle are estimated by the Kalman filter using three displacement (x, y, and z) and three velocity ($\dot{x}$, $\dot{y}$, and $\dot{z}$) sensors mounted on the mast-tip. The configuration of the actuators and sensors is collocated at both the shuttle and the mast-tip.

Several design parameters are tabulated in Table 1 for the estimator-based sliding-mode controller. The optimal weighting matrix is selected as

$$Q_s = \begin{bmatrix} \rho_r I^{6\times 6} & 0 \\ 0 & \rho_f \omega_i^2 \end{bmatrix}, \tag{52}$$

where $i = 1, \ldots, \iota$ and ι is the same as the order of the estimator. For the state estimation, it is initially assumed that the disturbances caused primarily by tangential and centrifugal forces are known in the controller and estimator designs. In the stage of evaluating the performance of the estimator-based sliding-mode controller, the disturbance terms are dropped in both the controller and estimator, but the time-varying effects of the system matrices such as stiffening and gyroscopic terms remain only in the estimator dynamics. In the case of slower angular motion, the stiffening and gyroscopic effects are smaller.

The influence term of the tracking model in equation (43) adopted a tangential force which can provide the effect for angular acceleration of the shuttle in the specific application to the SCOLE model. Of course, the influence term depends on the specific problem such that a designer could select a different one. During the numerical simulation, the first two modes are most significantly excited by the shaped input command in an

TABLE 1

Design parameters for the controller and estimator

Rigid-body feedback coefficient,	κ	1000
Global reaching coefficient,	ν	20
Rigid-body weighting coefficient,	ρ_r	20000
Elastic weighting coefficient,	ρ_f	1
Process noise intensity,	Q_p	$1{\cdot}0 \times 10^{-3} I^{\iota\times\iota}$ m
Measurement noise intensity,	Q_m	$1{\cdot}0 \times 10^{-4} I^{\iota\times\iota}$ m
Open-loop torque period,	Ω	4·0 rad/s

open-loop manner. In order to obtain no residual vibration, the second mode frequency of the tracking model is replaced with the first mode frequency because only the first mode is used for shaping the input. Therefore, the tracking model does generate four non-zero states and maintains the remaining states at zero.

The desired input command is shaped by a two-impulse sequence. Of course, more impulses can be used for the increment of robustness as well as the reduction of residual vibration. However, the control suffers from a longer operational time. Furthermore, there is a drawback of the input shaping technique in an on-line implementation of the multiple impulse sequence. It is difficult to design the amplitudes of the second impulse, the third impulse, and so on according to the estimated natural frequencies. For example, Tzes [16] used only a two-impulse sequence for the application of a single link arm to select a payload by estimating the first natural frequency in the frequency domain. In this paper, the on-line operation of the input shaping technique is not implemented. However, it is used to provide a faster operation, more efficient maneuvering, and a more reliable controller in a realistic and problematic circumstance.

All computations and plots shown in the paper were performed on an IBM RISC 6000 Workstation. The control schematic diagram which indicates the interactions between the commands, the ideal model, the sliding-mode controller, the SCOLE simulation, and the state estimation is shown in Figure 2. In the numerical simulation, four cases are compared from the aspect of antenna deflections and rotations. The four cases are as follows:

1. *Tracking control* (*a*) requires that most non-ideal effects are assumed to be known for the design of the ESMC and the time-varying Kalman filter. However, the ESMC does not include time-varying effects such as stiffening and gyroscopic terms. The ESMC attempts to follow the states of the ideal tracking model. The control efficiency is demonstrated in this case.
2. *Tracking control* (*b*) allows the most significant disturbances in the slewing maneuver to be dropped in the ESMC design and the time-varying Kalman filter to be dropped out of the tracking control (a) case. The disturbances are the tangential and centrifugal forces. The ESMC again tracks the states of the ideal tracking model. The robustness of the ESMC is illustrated in this case.
3. *Open-loop control* states that neither the ESMC nor the Kalman filter are involved. The input shaping technique is used to evaluate the performance with only a two-impulse sequence.
4. *Rigid-body control* says that the ideal tracking model is not used. The ESMC attempts to hold the flexible mast like a rigid body.

In all four cases, the input command has a magnitude $T_{amp} = 20\,\text{lbft}(2{\cdot}7651\,\text{kg}_f\text{m}\,)$ as shown in Figure 3 and it is shaped by a two-impulse sequence and then is applied to the shuttle for a 30° roll maneuver. The estimator-based sliding-mode controller is charged with rejecting perturbations during the entire slewing motion. The desired motion of the shuttle is shown in Figure 4 with the maximum velocity being around $6^\circ/\text{s}$.

The main control objective of the SCOLE model is to aim the antenna within a certain tolerance $0{\cdot}02^\circ$ in a short period of time. Hence, plots of the antenna rotations versus time are presented. Figures 5–7 illustrate the instantaneous antenna rotations with respect to $x_0y_0z_0$ axes respectively. The figures show the responses produced during the maneuver with all four of the control techniques. The effect of the tangential and centrifugal terms in the controller and estimator, in the case of tracking control (b), shows more angular displacement and it takes a longer period of time than does one of the tracking control (a)

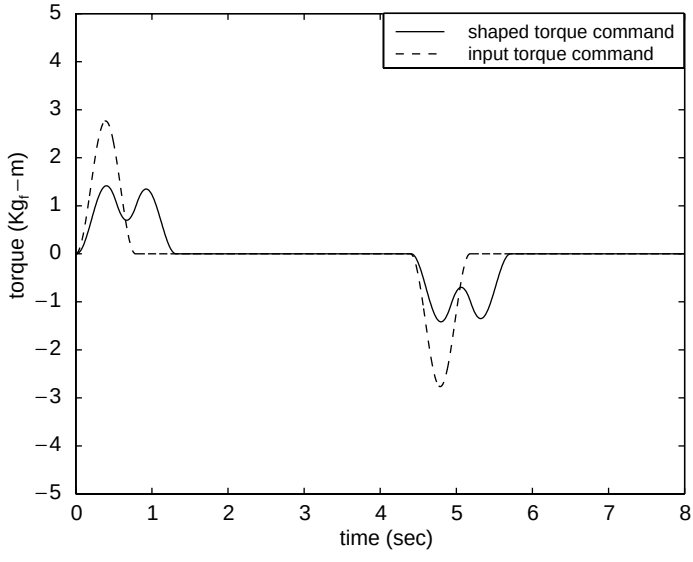

Figure 3. Command inputs for a 30° roll maneuver.

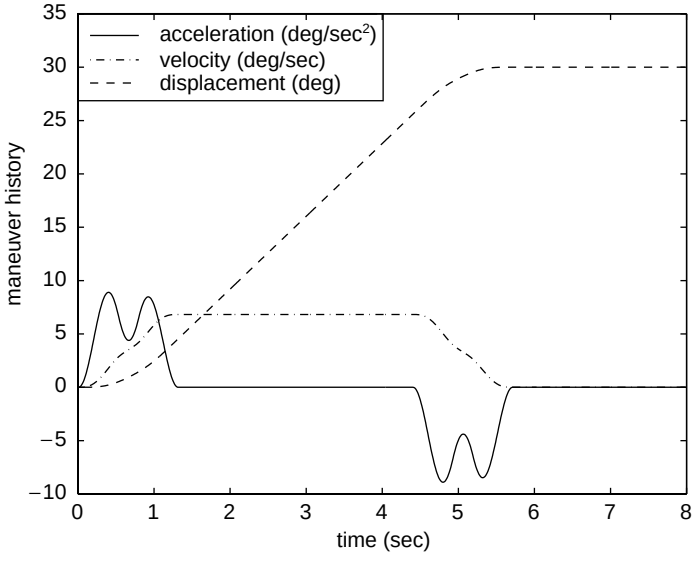

Figure 4. The maneuver strategy of the shuttle for a 30° roll maneuver.

to settle down the oscillatory deflection because the ESMC is employing a globally asymptotic reaching technique [7] as opposed to a rapid switching technique. Nevertheless, it does eventually and quickly damp out the residual oscillatory deflection of all axes in the presence of modelling errors in the tracking control (a).

The equation of control effort ($C.E.$) for Figures 8 and 9 is defined as

$$C.E. = \int_0^\infty u(t)^{\mathrm{T}} u(t)\,\mathrm{d}t. \tag{53}$$

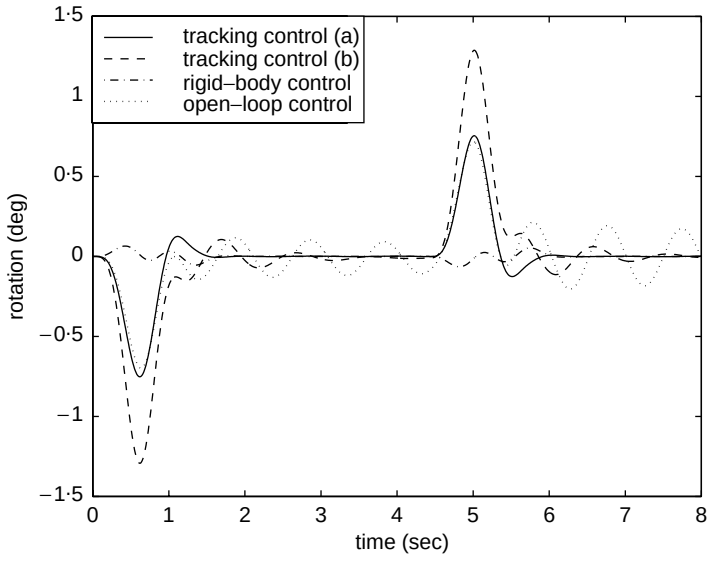

Figure 5. Antenna rotation at x_0 during a 30° maneuver.

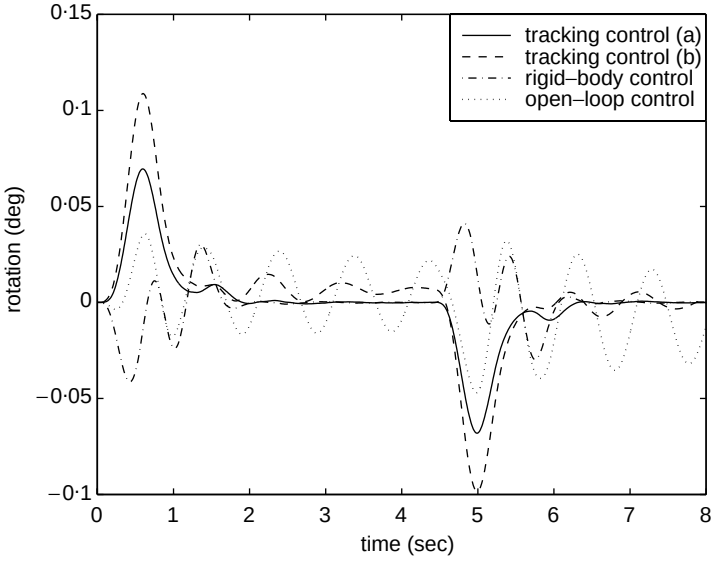

Figure 6. Antenna rotation at y_0 during a 30° maneuver.

The case of the rigid-body control is not very effective in controlling vibrations compared to the tracking control (a). The tracking control (b) requires more control effort than the other two cases. After 6 s, the tracking control (b) continuously consumes energy in order to damp out residual vibrations. The tracking control (a) required the least amount of control effort and is able to accomplish the 30° maneuver. The control effort for the entire system's operation in the tracking control (a) is a small quantity below $5(\text{lbft})^2$

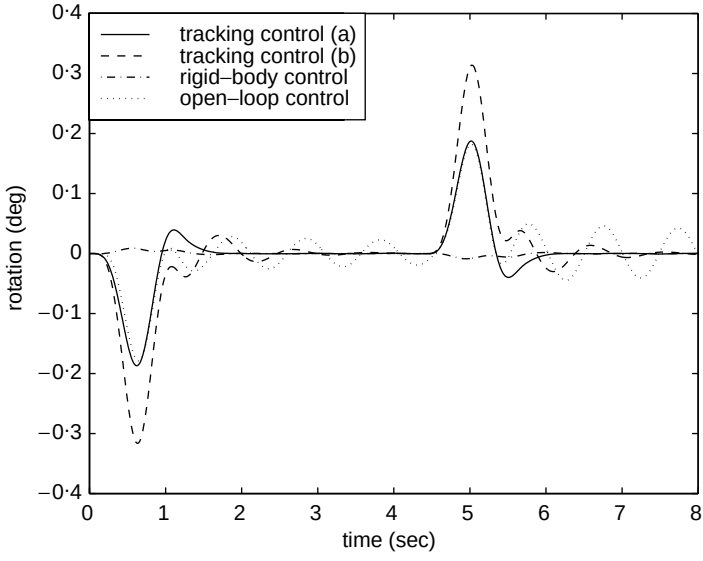

Figure 7. Antenna rotation at z_0 during a 30° maneuver.

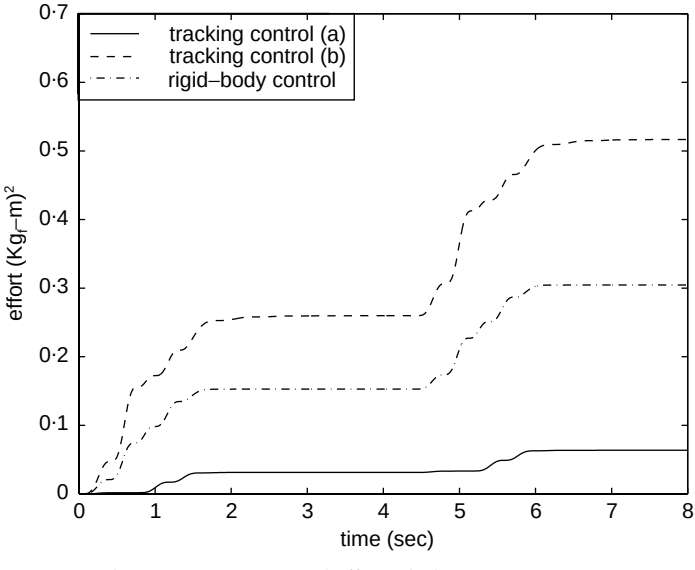

Figure 8. Torque control efforts during a 30° maneuver.

(0·4781 kg_f m) which are indirectly comparable to the results of reference [10]. They used either distributed force actuators or 10 discrete force actuators in controlling the vibration of the mast instead of using torque wheel actuators as noted in this paper. Each *C.E.* is for the entire operational effort.

Figures 10 and 11 are time-lapse plots of the spacecraft during the 30° roll maneuver with a plotting sampling time of 0·5 s. In the deformation plot, a scale factor of 10 is used to amplify the deformation for the plotting purpose. The view is from directly behind the spacecraft, showing the y_0z_0 plane with the x_0-axis directed into the paper. In each plotting

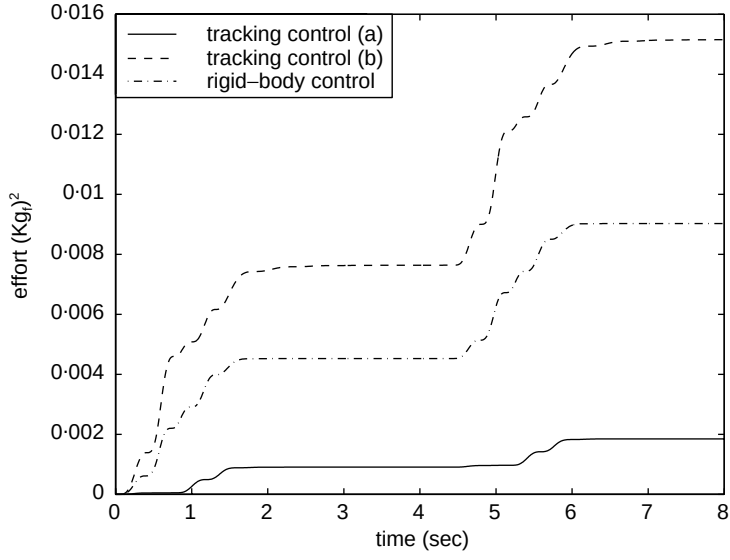

Figure 9. Force control efforts during a 30° maneuver.

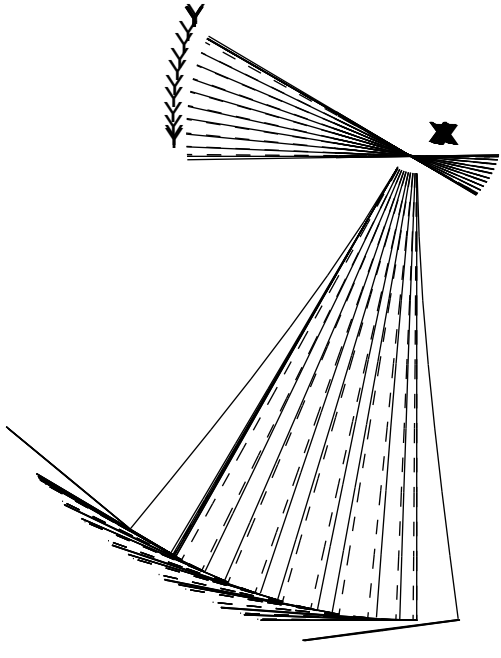

Figure 10. Time-lapse plot of 30° roll maneuver (input shaping technique).

sampling time, two plots appear, one is a dashed line representing the structure as if it is rigid, and the other is a solid line representing the deformed structure. Due to the tracking control strategy, the initial and ending oscillations in both cases appear to be similar. The mast continues to oscillate during the entire activity in the case of the input shaping

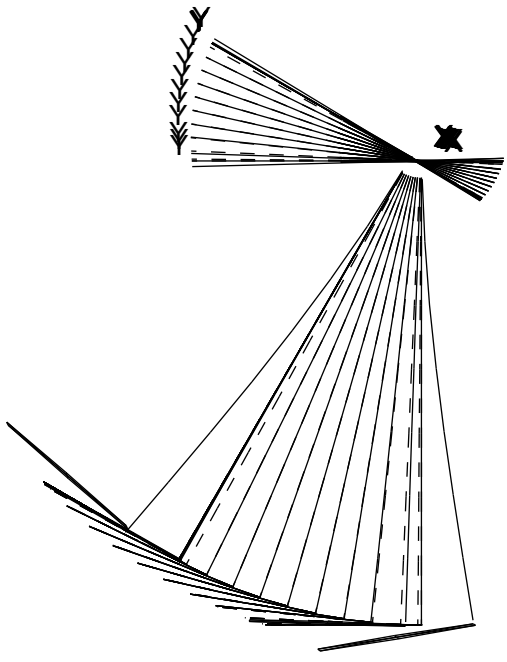

Figure 11. Time-lapse plot of 30° roll maneuver (tracking control (a)).

technique. However, in the tracking control (a) case, the mast is initially behind its undeformed position and then it bounces forward to precede to the desired configuration. During the coasting stage and at the end of the maneuver, the vibration of the mast is not noticeable.

In the 30° maneuver with a maximum angular velocity below 5°/s as shown in Figure 4 and the maximum applied torque 10 lbft(0·9562 kg_fm) on the shuttle as shown in Figure 3, the time-varying effect of the system dynamics is relatively small.

The tracking control (a) is tested for the zero damping case $C_r = 0^{l \times l}$ with the same design parameters as noted in Table 1. It turns out that the residual vibration of the mast exists at the end of the 30° slewing maneuver. However, the maximum vibration amplitude is below 0·02° which is the control objective of the SCOLE operation. It appears that the overall performance of the ESMC is similar to the non-zero damping case.

5. CONCLUSIONS

The ESMC is developed for a linear stochastic system with a known disturbance. The error states are determined using a Kalman filter to define the number of sliding hypersurfaces. The number of controller poles results from the thickness of the boundary layers and the remaining poles for the entire states are determined by the sliding hypersurface selection. The ESMC minimizes the expected value of a guadratic objective function composed of error states which always remain in the intersection of sliding hypersurfaces with respect to the remaining poles.

In a numerical simulation with the SCOLE model, the ESMC is modified due to the maneuvering of the rigid-body and combined with the ideal tracking model and the input

shaping technique for economical performance reasons. The first-mode tracking strategy is shown to be more efficient than the rigid-body motion strategy. With three torque wheel actuators and three displacement sensors and three velocity sensors at the mast-tip, the large angle maneuver is successfully accomplished without significant residual vibrations.

ACKNOWLEDGMENTS

We would like to thank Dr R. D. Quinn of The Case Western Reserve University, Cleveland, OH. He provided his FORTRAN code for the SCOLE model used in the paper which we gratefully appreciate.

REFERENCES

1. J.-J. E. Slotine 1985 *Journal of Robotics Research*, **4**, 49–64, The robust control of robot manipulators.
2. H. Öz and O. Mostafa 1988 *Journal of the Astronautical Sciences* **36**, 311–344. Variable structure control system (VSCS) maneuvering of flexible spacecraft.
3. K. D. Young and U. Özguner 1993 *Journal of Control* **57**, 1005–1019. Frequency shaping compensator design for sliding mode.
4. N. K. Gupta 1980 *Journal of Guidance, Control and Dynamics* **3**, 529–535. Frequency-shaped cost functionals: extension of linear-quadratic-Gaussian design methods.
5. A. Sinha and D. W. Miller 1995 *Journal of Guidance, Control, and Dynamics* **18**, 486–492. Optimal sliding-mode control of a flexible spacecraft under stochastic disturbance.
6. V. I. Utkin 1992 *Sliding Modes in Control Optimization*. New York: Springer-Verlag.
7. O. Mostafa and H. Öz 1989 *Journal of the Astronautical Sciences*. **37**, 529–550. Chatter elimination in variable structure control maneuvering of flexible spacecraft.
8. C. Edwards and S. K. Spurgeon 1998 *Sliding Mode Control: Theory and Aapplications*. PA: Taylor & Francis Inc.
9. W. L. Brogan 1991 *Modern Control Theory*. New Jersey: Prentice-Hall Inc.
10. L. Meirovitch and R. D. Quinn 1987 *Journal of Guidance, Control, and Dynamics* **10**, 453–465. Equation of motion for maneuvering flexible spacecraft.
11. C. J. Swigert 1980 *Journal of Guidance, Control, and Dynamics* **3**, 460–467. Shaped torque technique.
12. R. D. Quinn and L. Meirovitch 1986 *Proceedings of the AIAA/ASME/ASCE/AHS 27th Structures, Structural Dynamics and Materials Conference, Pt. 2*, 342–354, New York: AIAA, Equations for the vibration of a slewing flexible spacecraft.
13. J. L. Junkins and J. D. Turner 1986 *Optimal Spacecraft Rotational Maneuvers*. New York: Elsevier Science Publishers.
14. N. C. Singer and W. P. Seering 1990 *Journal of Dynamic Systems, Measurement, and Control* **112**, 76–82, Preshaping command inputs to reduce system vibration.
15. Y.-G. Sung and Y.-P. Park 1999 *KSME International Journal* **13**, 714–726. Model reduction of semi-positive definite systems reflected to actuator and sensor locations.
16. A. P. Tzes 1990 *Ph.D. Thesis, Ohio State University, Columbus, OH*. Self-tuning controllers for flexible link manipulators.